Human Molecular Genetics, 2021, Vol. 00, No. 00 1–8

https://doi.org/10.1093/hmg/ddab289
Advance Access Publication Date: 30 September 2021
General Article

GENERAL ARTICLE

Sensitive quantification of m.3243A>G mutational proportion in non-retinal tissues and its relationship with visual symptoms

Nathaniel K. Mullin†, Kristin R. Anfinson, Megan J. Riker, Kelsey L. Wieland, Nicole J. Tatro, Todd E. Scheetz, Robert F. Mullins, Edwin M. Stone and Budd A. Tucker*

Department of Ophthalmology and Visual Sciences, University of Iowa Institute for Vision Research, Iowa City, IA 52242, USA

*To whom correspondence should be addressed at: Department of Ophthalmology and Visual Sciences, University of Iowa Institute for Vision Research, Iowa City, IA 52242, USA. Tel: +(319) 353-4488; Fax: +(319) 335-7241; Email: budd-tucker@uiowa.edu

Abstract

The m.3243A>G mutation in the mitochondrial genome commonly causes retinal degeneration in patients with maternally inherited diabetes and deafness and mitochondrial encephalopathy, lactic acidosis and stroke-like episodes. Like other mitochondrial mutations, m.3243A>G is inherited from the mother with a variable proportion of wild type and mutant mitochondrial genomes in different cells. The mechanism by which the m.3243A>G variant in each tissue relates to the manifestation of disease phenotype is not fully understood. Using a digital PCR assay, we found that the % m.3243G in skin derived dermal fibroblasts was positively correlated with that of blood from the same individual. The % m.3243G detected in fibroblast cultures remained constant over multiple passages and was negatively correlated with mtDNA copy number. Although the % m.3243G present in blood was not correlated with severity of vision loss, as quantified by Goldmann visual field, a significant negative correlation between % m.3243G and the age of onset of visual symptoms was detected. Altogether, these results indicate that precise measurement of % m.3243G in clinically accessible tissues such as skin and blood may yield information relevant to the management of retinal m.3243A>G-associated disease.

Introduction

Maternally inherited diabetes and deafness (MIDD) [MIM: 520000], mitochondrial encephalopathy, lactic acidosis and stroke-like episodes (MELAS) [MIM: 540000] and Leigh syndrome [MIM: 256000] are all multi-tissue syndromic diseases most often caused by a common single nucleotide variant in the mitochondrial tRNA gene *MT-TL1*. This variant is an A>G substitution at position 3243 on the mitochondrial chromosome (m.3243A>G) (1,2). While this variant can cause a constellation of symptoms such as those traditionally described in MIDD and MELAS, it is also known to cause a variable presentation between even related individuals that can impede molecular detection and proper diagnosis (3,4). Further complicating the understanding of the genotype-phenotype connection in m.3243A>G disease is the fact that this variant is likely more common among the unaffected population than might be expected given its sometimes severe phenotype (5). The basis for the variety of phenotypes caused by this variant, both in terms of severity and which organs are affected in different patients, is not well understood (6). Beyond the impact of background variants that likely play a disease modulating role in many rare

†Nathaniel K. Mullin, http://orcid.org/0000-0003-4320-2852
Received: August 6, 2021. **Revised:** September 22, 2021. **Accepted:** September 24, 2021

genetic diseases (7), the genetics of diseases caused by variants in the mitochondrial genome are complicated by the peculiar mode of inheritance of the mitochondrial chromosome during cell division.

The mitochondrial DNA (mtDNA), found within the mitochondrial matrix, is a relatively small (~16kbp) circular piece of double stranded DNA (8). This chromosome encodes the genes of 13 proteins, 22 tRNAs and 2 rRNAs; only a small fraction of the more than one thousand genes responsible for the structure and function of the human mitochondrion (8). Each mitochondrion may contain between 1 and 15 copies of this genome, and each human cell contains hundreds to thousands of mitochondria (9). As such, there exist many more copies of the mitochondrial genome than the two copies of the nuclear genomes typically present in any one eukaryotic cell. Given the high copy number of mtDNA, there may exist within a single cell a mixture of mutant and wild-type mitochondrial alleles. This phenomenon is known as heteroplasmy and is appreciated as playing a role in the manifestation of mitochondrial genetic disease (10).

How heteroplasmy is managed by the cell and what role it plays in cellular and tissue dysfunction in disease states are currently active areas of interest in mitochondrial disease (11–13). However, the unique mode of heredity of mitochondrially encoded genes may be, at least in part, an explanation for the striking heterogeneity in phenotypic expressivity in the m.3243A>G diseases (14).

In order to better understand how precise mitochondrial genotyping (i.e. measuring allelic proportions within a sample) relates to clinical presentation of mitochondrial genetic disease, we studied a collection of patients with clinically diagnosed and molecularly confirmed m.3243A>G disease. To precisely, inexpensively and rapidly quantify the ratio of mutant to wild-type mitochondrial genomes in patient samples, we developed an m.3243 allele-specific digital PCR assay. Employing this assay on two easily accessible tissues, skin and whole blood, we were able to correlate the % m.3243G with visual symptoms in affected patients. We further demonstrate that the % m.3243G remained constant in the cells of an individual across multiple divisions and negatively correlated with mtDNA copy number in dermal fibroblasts. Altogether, this work contributes to the growing understanding of the mitochondrial genotype-phenotype relationship in m.3243A>G-associated disease.

Results

To determine the proportion of mutant to wild-type m.3243 alleles present in primary patient samples, a digital PCR assay, similar to that reported by Klein Gunnewiek *et al.* (15), was developed (Fig. 1A). Dermal fibroblasts and whole blood recovered from a cohort of MIDD and MELAS patients (Table 1) were evaluated. These patients all had clinically diagnosed retinal disease and had been previously identified as carrying the m.3243A>G variant. A representative plot showing ~16 000 reaction wells from a single dPCR run is shown (Fig. 1B). The specificity of the m.3243A/G dPCR assay was confirmed by running the assay on DNA isolated from five dermal fibroblast lines from individuals across five decades of life not known to carry the m.3243A>G mutation (Fig. 1C). As expected, the m.3243G allele was not detected in any of these control samples.

Using digital PCR, we observed that the % m.3243G present in blood and skin derived dermal fibroblasts varied drastically between individuals within our cohort. Specifically, the proportion of m.3243G ranged from 13 to 81% in dermal fibroblasts and 5 to 41% in blood. We sought to determine whether

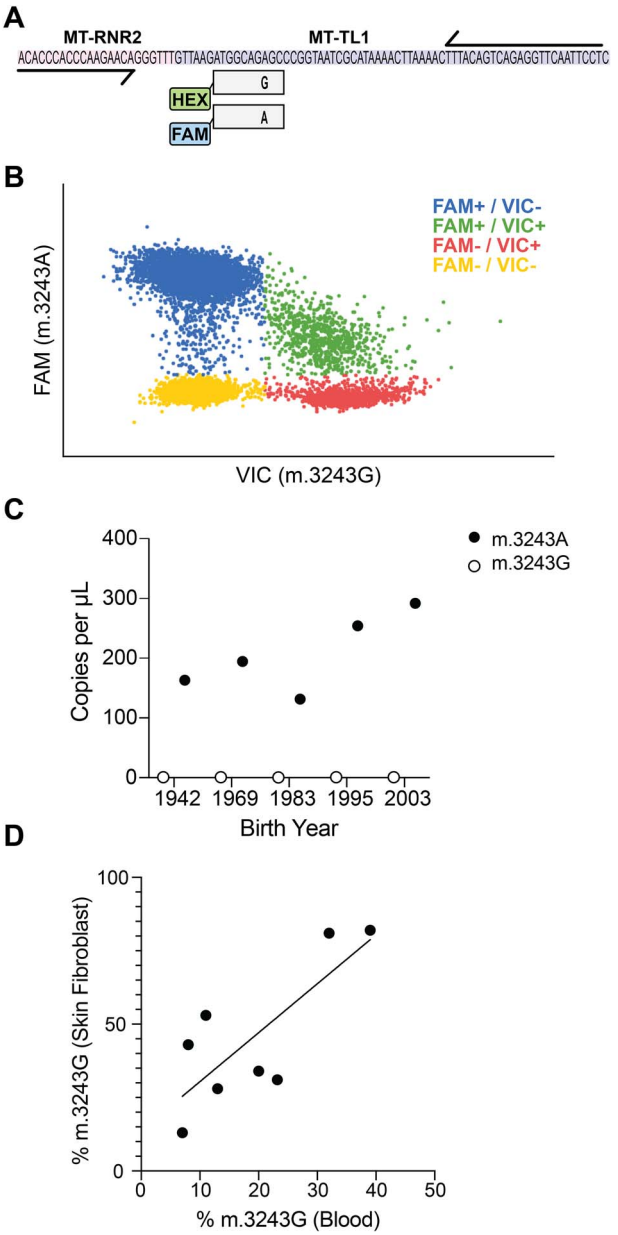

Figure 1. Measurement of m.3243A>G proportion in peripheral tissues of MIDD patients. (**A**) Schematic of allele-specific digital PCR assay for m.3243. (**B**) Representative plot showing results of m.3243A>G dPCR assay. (**C**) Copies of m.3243A (wild-type) and m.3243G (mutant) detected by dPCR in skin fibroblast samples from patients without m.3243A>G disease. No m.3243G allele is detected. (**D**) The m.3243A>G proportion in the blood and skin fibroblasts from the same MIDD patient is positively correlated. Notably, blood concentration is consistently lower than skin fibroblast concentration for any given individual.

this range represented a random segregation of mitochondria and mitochondrial alleles during tissue specification in early development, or if there was a cell type-level control of wild-type m.3243A to mutant m.3243G. By plotting the proportion of m.3243A>G in dermal fibroblasts versus blood for each patient from which we had both sample types, we observed a strong correlation between the two sample types across the cohort (P-value = 0.023, R^2 = 0.6055) (Fig. 1D). This finding is supported by previous studies that observed a correlation of m.3243A>G proportion in muscle and urinary epithelial cells from the same

Table 1. Summary of m.3243A>G patient cohort clinical and molecular data

Patient Number	IP-15-32-1	MP-1349-1	19-B-1	MP-1174-1	CRD-400-1	IP-15-34-1	MP-1685-1	MP-1678-1	MP-1734-1	MP-1712-1	MP-1727-1	101-I-2
Gender	Female	Female	Male	Female	Female	Female	Female	Female	Female	Female	Female	Male
Age at visit (years)	27	31	41	41	56	59	59	64	63	65	41	65
Vision (years)	21	32	36	32	56	49	59	63	35	40	41	50
Hearing (years)	21	44	8	39	n/a	49	30	53	58	n/a	n/a	44
Diabetes (years)	n/a	36	14	34	n/a	52	40	n/a	25	n/a	n/a	37
Initial diagnosis	MELAS	Pattern Dystrophy / Inflam-matory Injury	MELAS	Pattern Dystrophy	ABCA4 / RDS	Hereditary Retinal Dystrophy	MIDD	Nummular Choroidal Atrophy	Autosomal Dominant Macular Dystrophy	Sjogren's Reticular Pattern Dystrophy / Angioid Streaks	Occult Macular Dystro-phy/ RDS with no Family History	Heritable Macular Dystro-phy with Hearing Loss
Family History	n/a	Diabetes (grand-mother, mother), Macular Disease (grand-mother)	Sister, Mother	Diabetes, Hearing Loss	n/a	Brother, Mother	Siblings, Mother, Daughter	n/a	Hearing Loss	n/a	n/a	Hearing Loss
% m.3243G (Blood)	39	20	32	23	13	11	8	7	17	20	19	24
% m.3243 (HDF)	82	34	81	31	28	53	43	13	n/a	n/a	n/a	n/a
mtDNA Copy Number (HDF)	982.72	2832.81	1151.28	2118.92	2716.67	1229.84	2201.16	2031.57	n/a	n/a	n/a	n/a

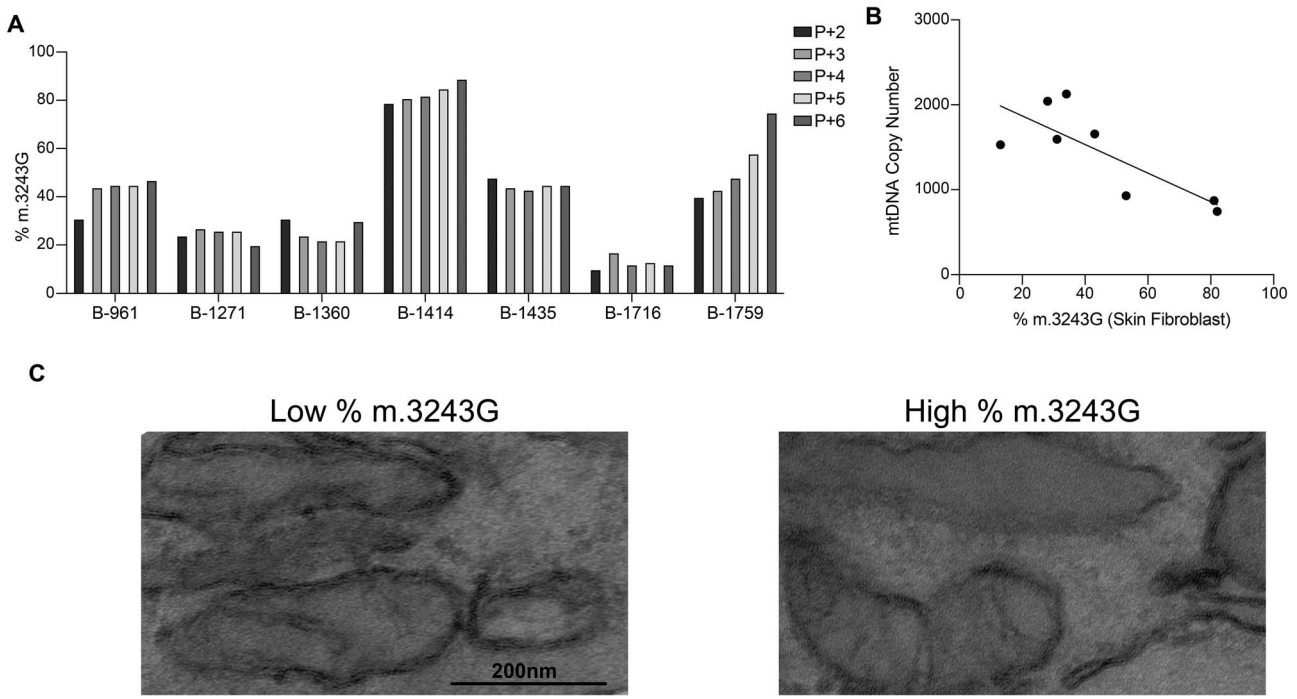

Figure 2. The dynamics and effects of m.3243A>G proportion in cultured dermal fibroblasts. (**A**) The proportion of m.3243G allele is generally stable in dermal fibroblast across multiple passages. (**B**) The m.3243A>G proportion negatively correlates with mtDNA copy number in dermal fibroblasts from MIDD patients. (**C**) Mitochondria in dermal fibroblasts from patients with m.3243A>G disease have dilated mitochondria with a reduction in cristae.

patient (16). We observed that the % m.3243G in dermal fibroblasts was consistently higher than that of blood, implying cell-type-specific management of pathogenic mitochondrial allele accumulation and replication.

To assess the stability of the m.3243 allele as a function of cell division (i.e. % mutant to wild-type), we expanded patient-derived dermal fibroblasts *in vitro* and performed dPCR. As shown in Figure 2A, the % m.3243G did not significantly change across five serial passages for either of the cell lines evaluated. The variation between cell lines (*P*-value < 0.0001) was more remarkable than that within lines over serial passage (*P*-value $= 0.1893$). This result indicates that the % m.3243G in patient-derived dermal fibroblasts is subject to neither positive nor negative selection in a routine cell culture system.

In addition to measuring the proportion of m.3243A>G in fibroblast cultures, we also measured mitochondrial DNA (mtDNA) copy number per cell using a separate digital PCR assay (see Materials and Methods). We found that mtDNA copy number in cultured dermal fibroblasts ranged from 982.72 to 2832.81 copies per diploid nuclear genome, a surrogate measurement for cell number. When we plot mtDNA copy number against m.3243A>G proportion for each of the eight MIDD patient cell lines, we observed a negative correlation in which higher proportion of mutant alleles correlated with a lower mtDNA copy number (*P*-value $= 0.019$, $R^2 = 0.6257$) (Fig. 2B).

Finally, we examined the impact of the % m.3243G in cultured cells on mitochondria ultrastructure using transmission electron microscopy (TEM) (Fig. 2C). Mitochondria in the fibroblasts obtained from patients with m.3243A>G-associated disease were dilated with abnormal cristae (a structural phenotype that was previously described in tissues from patients with mitochondrial genetic disease (17)).

To determine if there is a relationship between visual phenotype and % m.3243G present in clinically accessible tissues, first we quantified the Goldmann visual fields of 12 patients with molecularly confirmed m.3243A>G-associated disease obtained at their first visit. The m.3243A>G variant is known to cause a characteristic macular atrophy in the retina of affected individuals with relative sparing of the peripheral retina (18). Interestingly, we found no correlation between % m.3243G in blood and preserved visual field at the first presentation (*P*-value $= 0.977$, $R^2 = 0.0000$) (Fig. 3A).

Discussion

Previous studies have demonstrated that the % m.3243G present in blood negatively correlates with age of onset of diabetes in MIDD (19). As a surrogate for the aggressiveness of retinal manifestations of m.3243A>G disease, we used the age of onset of visual symptoms for each patient (Table 1). We plotted the age of onset of visual symptoms versus % m.3243G in blood (Fig. 3B) and cultured dermal fibroblasts (Fig. 3C). A significant negative correlation between % m.3243G present in blood and age of onset of visual symptoms was identified ($P = 0.004$, $R^2 = 0.7292$). While the correlation between the % m.3243G in cultured dermal fibroblasts and age of visual symptom onset did not reach statistical significance, a negative trend was observed (*P*-value $= 0.106$, $R^2 = 0.3768$).

The unique genetics of the mitochondrial chromosome obscure the genotype-phenotype relationship in the m.3243A>G family of diseases. However, without a more complete understanding of this relationship and the mechanisms underpinning it, we will remain unable to adequately design treatments and prognostic tools for disease such as MIDD, MELAS and Leigh Syndrome. A major question associated with m.3243A>G disease is, why does phenotype present in such a heterogenous manner between patients, both in terms of which organs are involved and how severe tissue damage is? Prevailing thought on the mechanism to answer this question relies primarily on two assumptions: (i) that there is a required threshold of

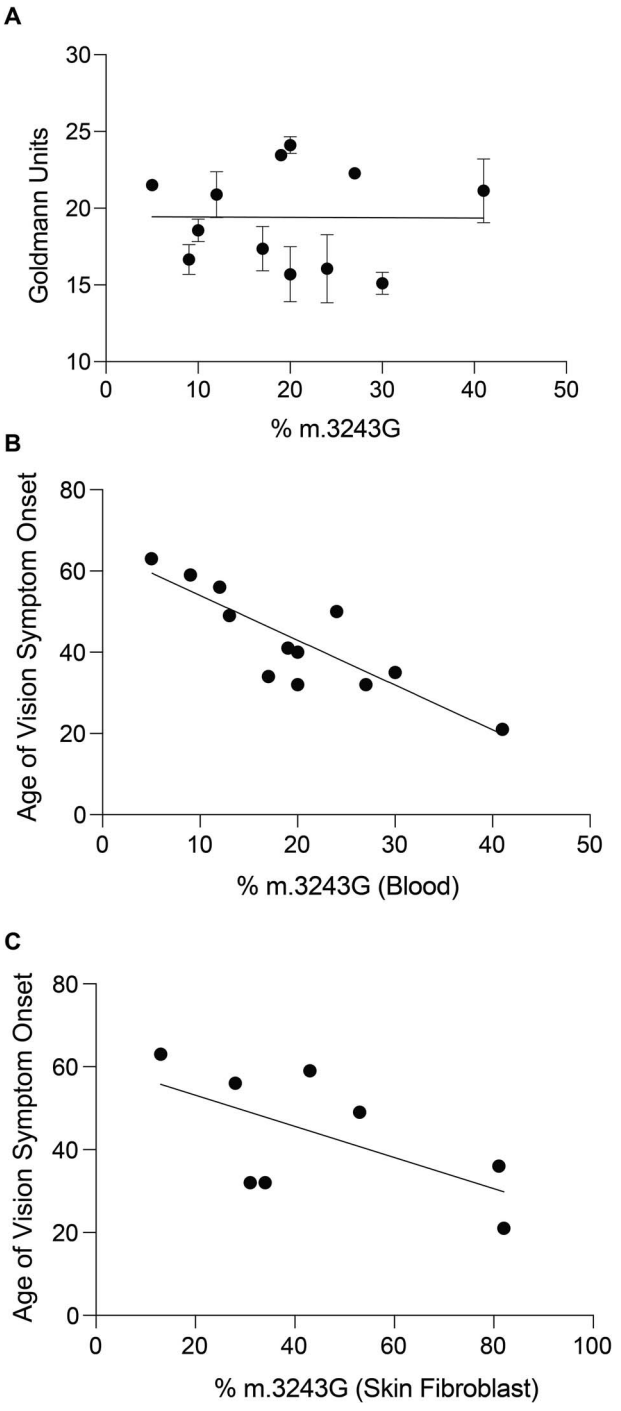

Figure 3. Comparison of % 3243G with visual disease phenotype. (**A**) No correlation was observed between the cumulative visual field area (as measured in Goldmann Units) and the proportion of m.3243A>G in blood. The average area between both eyes is shown, with error bars representing the range. (**B**) The proportion of mutant m.3243G allele in blood negatively correlates with the age of onset of visual symptoms in MIDD patients. (**C**) A non-significant negative correlation is observed between the proportion of mutant m.3243G allele in skin and the age of onset of visual symptoms in patients with m.3243A>G-associated disease.

mitochondrial function that is cell type specific and (ii) that mutant mitochondrial alleles segregate into tissues randomly during development.

The first assumption posits that there is a minimal threshold of mitochondrial activity (presumably tied to energy production) beneath which cells become dysfunctional (10). This threshold may vary depending on the energy needs of different cell types. In relation to m.3243A>G, this threshold model says that if cells surpass a certain proportion of mutant to wild-type mitochondria, they will become dysfunctional and cause tissue damage. This concept is supported by previous work in cybrid cell lines with specified m.3243A>G levels, in which investigators observed stereotypic changes in cellular metabolism associated with an increase in the % of m.3243G alleles present (20–22).

The second assumption in the prevailing framework is determined through random segregation in the cell divisions of early embryological development. This is the proposed explanation for why some people with m.3243A>G disease experience involvement of many organs, while in others disease is restricted to one or two. However, a case study of monozygotic twins with MELAS caused by m.3243A>G found that the segregation of mutant allele among tissues was the same in both twins, indicating that this process is not purely random (23). On a tissue-level, the segregation of the m.3243A>G variant has been shown to vary between different cell types within a tissue (24) and the proportion of other mitochondrial variants has been shown to be non-randomly distributed between regions within the same organ (25).

Overall, our data indicate that mechanisms underlying m.3243A>G pathogenesis may be more complex than currently appreciated. In our fibroblast experiments, we found that the proportion of mutant genomes is stable across repeated passages. Interestingly, this finding is counter to previous studies of transmitochondrial cell lines in which mitochondria harboring m.3243A>G were experimentally inserted into cells lacking the organelle (26). As these earlier experiments used a transplant of pathogenic variant into a wild-type cell, the incongruity of our findings suggests a possible role for nuclear genetics in the maintenance of stable m.3243A>G proportion. In sum, passage number of cultured fibroblasts does not appear to confound measurements of m.3243A>G proportion in most cell lines, an important consideration looking forward to *in vitro* modeling of m.3243A>G-associated disease. Defining the exact pathogenic mechanism of m.3243A>G in the retina will require isolation of cell types and precise manipulation of heteroplasmy *in vitro*. One promising approach that is well-suited to these requirements is the use of induced pluripotent stem cells to generate affected cell types in isolation and with controlled % m.3243G (15,27).

We found a pattern in correlation of m.3243A>G proportion between dermal fibroblasts and blood from the same affected individual (Fig. 1D). While these cell types are both derived of mesoderm lineage, the fact that the levels correlate and that skin fibroblasts have a consistently higher m.3243A>G proportion indicates that a cell-type-specific mechanism for m.3243A>G proportion control may limit the proportion of mutant genomes in blood cells. Furthermore, the fact that the % of m.3243G present was stable across cell divisions indicates that different cells may maintain or regulate heteroplasmy by some mechanism. Indeed, tissue and even cell-type-specific selection of mtDNA variants has been demonstrated previously in animal models and patients (24,28,29). The mechanisms that govern heteroplasmy in the retina and how the proportion of m.3243G in that tissue relates to that of dermal fibroblasts and blood in affected individuals is still not understood. Although donor tissue from MELAS or MIDD patients is rare, our understanding of this disease will benefit from identifying cell-type-specific

patterns of heteroplasmy from both donor tissue and disease-specific iPSC derived cell types.

As has been noted in other tissues affected in MIDD and MELAS (30), we found that the proportion of mutant alleles in peripheral blood negatively correlates with age of onset of retinal disease. Specifically, the greater the % m.3243G, the earlier the patient presented with visual defects. Previous studies have also found a relationship between peripheral % m.3243G and severity of disease (31) as well as a correlation between m.3243A>G proportion and mtDNA copy number (32). The relationship between mtDNA copy number and cellular function in the context of m.3243A>G mutation has been previously investigated (26). Altogether, these connections invoke a model for genotype-phenotype correlation in which heteroplasmy is controlled through some patient-level mechanism, as opposed to a model of random segregation of mutant mitochondrial genomes into tissues during development. Previous studies of families with m.3243A>G disease have shown that patterns of phenotype expressivity are heritable, implying a role for nuclear genetics in determining m.3243A>G phenotype independent of heteroplasmy (6). Our findings also highlight the importance of accurate measurement of m.3243A>G proportion in the molecular diagnosis of MIDD and MELAS patients. While visual field size does not correlate with m.3243G proportion in peripheral tissue, this may indicate an artifact of patient presentation rather than lack of connection between peripheral tissues and retinal health. Visual fields were measured from the first visit for each patient regardless of age. As such, we believe that visual field measurements represent the level of vision loss required for patients to seek treatment rather than an indication of % m.3243G.

Like many other presumed monogenic diseases of the retina and other tissues, the phenotype of the m.3243A>G family of disease may be governed by factors beyond the presence of a single variant. The role of nuclear genetic background in m.3243A>G pathogenesis is obscured by varying heteroplasmy between tissues and cells but is an important area of current investigation. Ultimately, identifying compensatory mechanisms and other nuclear or mitochondrial genetic factors that govern which tissues are affected in m.3243A>G-associated disease would dramatically improve the clinical management of these conditions. Knowledge of such mechanisms would also aid treatment of these diseases, whether through gene replacement, or augmentation of pathways that control the proportion of mutant alleles and total number of mitochondria. Overall, the current study contributes to the growing appreciation for the m.3243A>G-associated diseases as complex but largely non-random genetic conditions and sheds light on specifically the retinal manifestations of these syndromes.

Materials and Methods

Human subject consent

This study was approved by the institutional review board of the University of Iowa and adhered to the tenets set forth in the Declaration of Helsinki. All study subjects provided written informed consent and were enrolled at the University of Iowa, Department of Ophthalmology and Visual Sciences.

Cell culture

Human dermal fibroblast (HDF) cells were isolated from 3 mm dermal punch biopsies via explant culture as described previously (33). Cells were cultured in MEM-α (Gibco) with 10% fetal bovine serum (Atlas Biologicals) and antibiotics (Primocin) at 37°C in a humidified incubator at 15% oxygen and confirmed negative for mycoplasma by luciferase assay (Lonza). Cultures were routinely passaged at a ratio of 1:10 using TrypLE dissociation reagent (Gibco).

DNA isolation

DNA was isolated from cultured fibroblasts using the Macherey-Nagel NucleoSpin kit following manufacturer's instructions. Nucleic acid quantity and quality were assessed using a Nanodrop spectrophotometer prior to downstream applications. DNA was diluted to appropriate concentration in water and stored at −20°C. DNA from blood samples was extracted by using the manufacturer's specifications for whole-blood DNA extraction using Gentra System's Autopure LS instrument (Valencia, CA).

Genotyping by digital PCR

Custom probe-based assays were designed against either variant at the m.3243 locus by Integrated DNA Technologies. Probes were designed incorporating several locked nucleic acids (indicated with '+' below) in order to attain adequate binding specificity to provide allelic specificity. For the mtDNA copy number assay, a probe-based assay was designed to target MT-ND2 using the IDT PrimerQuest online application. NCBI Primer Blast was used to check the specificity of each assay to the desired region. To target the nuclear genome, an assay specific to the RNAseP gene was used (Applied Biosystems Ref. 4401631).

Digital PCR was carried out using the Applied Biosystems 3D PCR platform. For the m.3243A/G assay, the following mixture was used (per reaction): 8.7 µL 3D Master Mix V2 (Applied Biosystems #A26358), 0.85 µL A-FAM Probe (5 µM), 0.85 µL G-HEX Probe (5 µM), 1.67 µL F Primer (5 µM), 1.67 R Primer (5 µM), 1.66 µL H2O and 2 µL DNA (0.1 ng/µL). For the mtDNA Copy Number Assay, the following mixture was used (per reaction): 8.7 µL 3D Master Mix, 0.85 µL MT-ND2-FAM Probeset (5 µM), 0.85 µL RNaseP-HEX Probe (5 µM) and 1.75 µL DNA (0.1 or 1 ng/µL), with H2O to 17.4 µL. For blood samples, 1 ng/µL DNA was used for the mtDNA Copy Number Assay and for skin samples 0.1 ng/µL DNA was used. In both assays, 14.5 µL of the mixture was loaded into a 3D Digital PCR chip using the QuantStudio Digital PCR Chip Loaded following the manufacturer's instruction.

The thermal cycler program was run as follows for the m.3243A/G assay: Step 1: 95°C—10 min; Step 2: 56°C—2 min; Step 3: 98°C—30 s and Step 4: 60°C—2 min, with steps 2 and 3 cycled 45 times. The thermal cycler program was run as follows for the mtDNA copy number assay: Step 1: 95°C—10 min; Step 2: 58°C—2 min; Step 3: 98°C—30 s and Step 4: 60°C—2 min, with steps 2 and 3 cycled 45 times. After amplification, chips were allowed to equilibrate to room temperature for ∼10 min and were then read. Data were analyzed using the 3D Quantstudio cloud-based web application, and the automatically generated thresholds were used.

The proportion of G allele for the *MT-TL1* A/G heteroplasmy assay was calculated as: (Copies/microliter (VIC))/(Copies/microliter (VIC) + Copies/microliter (FAM). The mtDNA copy number per nuclear genome was calculated as Copies/microliter (FAM)/(Copies/microliter (VIC)/2).

Probe Name	Color	F Primer	R Primer	Probe
MT-TL 3243 A	FAM	ACACCCACCCAAGAACA	AGGAATTGAACCTCTGACTGTAAA	AT+GG+CA+G+A+GC
MT-TL 3243 G	HEX	ACACCCACCCAAGAACA	AGGAATTGAACCTCTGACTGTAAA	ATGGCA+G+G+GC
MT-ND2	FAM	GAGGAGGGTGGATGGAATTAAG	CTACCGCATTCCTACTACTCAAC	AACTCCAGCACCACGACCCTACTA
RNase P	VIC	Proprietary (Applied Biosystems Ref. 4401631)		

Transmission electron microscopy

Dermal fibroblasts were cultured as described above in 12-well tissue culture-treated plates. At 80% confluence, cells were fixed in ½ strength Karnovsky's fixative and processed for TEM as described previously (34). Sections were cut at 85 nm with an ultra-microtome (Leica) and collected on copper slot grids coated with Formvar (0.5%) and images collected on a Hitachi HT7800 transmission electron microscope.

Goldmann visual field quantification

A locally developed method was used to quantify the volume of the hill of vision, based upon Goldmann kinetic perimetry. In brief, first, a digitized copy of the field was annotated using the TruthMarker App for iOS (35). Missing isopters (e.g. V4e) were computed by assuming the same proportion of loss relative to a normal field (36) as an isopter that was assessed at that visit (typically I4e). A custom program based upon the works of Weleber and Tobler (37) and Christoforidis (38) was used to compute the volume of the visual field, based upon the annotated fields. For patients with multiple visits, the visit with fields most representative of their visual function (typically their first visit) was selected for quantification.

Statistical analysis

All data were plotted and analyzed using Prism 9 (GraphPad). Where indicated, Pearson correlation was computed, and a two-tailed *P*-value was generated. R^2 and *P*-value are reported, and the best-fit linear regression line is plotted. For the fibroblast serial passaging experiment, two-way ANOVA was performed and resulting *P*-values for row and column factors are reported.

Acknowledgements

We would like to thank the patients and their families who agreed to participate in this study.

Conflict of Interest statement. The authors declare no competing interests.

Funding

National Institutes of Health (T32-GM008629, T32-GM007337, P30-EY025580).

References

1. Goto, Y., Nonaka, I. and Horai, S. (1990) A mutation in the tRNA(Leu)(UUR) gene associated with the MELAS subgroup of mitochondrial encephalomyopathies. *Nature*, **348**, 651–653.
2. Sakuta, R., Goto, Y.-I., Horai, S. and Nonaka, I. (1993) Mitochondrial DNA mutations at nucleotide positions 3243 and 3271 in mitochondrial myopathy, encephalopathy, lactic acidosis, and stroke-like episodes: a comparative study. *J. Neurol. Sci.*, **115**, 158–160.
3. Chin, J., Marotta, R., Chiotis, M., Allan, E.H. and Collins, S.J. (2014) Detection rates and phenotypic spectrum of m.3243A>G in the MT-TL1 gene: a molecular diagnostic laboratory perspective. *Mitochondrion*, **17**, 34–41.
4. Dvorakova, V., Kolarova, H., Magner, M., Tesarova, M., Hansikova, H., Zeman, J. and Honzik, T. (2016) The phenotypic spectrum of fifty Czech m.3243A>G carriers. *Mol. Genet. Metab.*, **118**, 288–295.
5. Manwaring, N., Jones, M.M., Wang, J.J., Rochtchina, E., Howard, C., Mitchell, P. and Sue, C.M. (2007) Population prevalence of the MELAS A3243G mutation. *Mitochondrion*, **7**, 230–233.
6. Pickett, S.J., Grady, J.P., Ng, Y.S., Gorman, G.S., Schaefer, A.M., Wilson, I.J., Cordell, H.J., Turnbull, D.M., Taylor, R.W. and McFarland, R. (2018) Phenotypic heterogeneity in m.3243A>G mitochondrial disease: the role of nuclear factors. *Ann. Clin. Transl. Neurol.*, **5**, 333–345.
7. Rahit, K. and Tarailo-Graovac, M. (2020) Genetic modifiers and rare Mendelian disease. *Genes (Basel)*, **11**, 329.
8. Larsson, N.G. and Clayton, D.A. (1995) Molecular genetic aspects of human mitochondrial disorders. *Annu. Rev. Genet.*, **29**, 151–178.
9. Satoh, M. and Kuroiwa, T. (1991) Organization of multiple nucleoids and DNA molecules in mitochondria of a human cell. *Exp. Cell Res.*, **196**, 137–140.
10. Stewart, J.B. and Chinnery, P.F. (2015) The dynamics of mitochondrial DNA heteroplasmy: implications for human health and disease. *Nat. Rev. Genet.*, **16**, 530–542.
11. Stefano, G.B. and Kream, R.M. (2016) Mitochondrial DNA heteroplasmy in human health and disease. *Biomed Rep*, **4**, 259–262.
12. Nissanka, N. and Moraes, C.T. (2020) Mitochondrial DNA heteroplasmy in disease and targeted nuclease-based therapeutic approaches. *EMBO Rep.*, **21**, e49612.
13. Wallace, D.C. and Chalkia, D. (2013) Mitochondrial DNA genetics and the heteroplasmy conundrum in evolution and disease. *Cold Spring Harb. Perspect. Biol.*, **5**, a021220.
14. DiMauro, S., Schon, E.A., Carelli, V. and Hirano, M. (2013) The clinical maze of mitochondrial neurology. *Nat. Rev. Neurol.*, **9**, 429–444.
15. Klein Gunnewiek, T.M., Van Hugte, E.J.H., Frega, M., Guardia, G.S., Foreman, K., Panneman, D., Mossink, B., Linda, K., Keller, J.M., Schubert, D. *et al.* (2020) M.3243A > G-induced mitochondrial dysfunction impairs human neuronal development and reduces neuronal network activity and synchronicity. *Cell Rep.*, **31**, 107538.
16. McDonnell, M.T., Schaefer, A.M., Blakely, E.L., McFarland, R., Chinnery, P.F., Turnbull, D.M. and Taylor, R.W. (2004) Noninvasive diagnosis of the 3243A > G mitochondrial DNA

mutation using urinary epithelial cells. *Eur. J. Hum. Genet.*, **12**, 778–781.
17. Vincent, A.E., Ng, Y.S., White, K., Davey, T., Mannella, C., Falkous, G., Feeney, C., Schaefer, A.M., McFarland, R., Gorman, G.S. *et al.* (2016) The Spectrum of mitochondrial ultrastructural defects in mitochondrial myopathy. *Sci. Rep.*, **6**, 30610.
18. Coussa, R.G., Parikh, S. and Traboulsi, E.I. (2021) Mitochondrial DNA A3243G variant-associated retinopathy: current perspectives and clinical implications. *Surv. Ophthalmol.*, **66**, 838–855.
19. Laloi-Michelin, M., Meas, T., Ambonville, C., Bellanne-Chantelot, C., Beaufils, S., Massin, P., Vialettes, B., Gin, H., Timsit, J., Bauduceau, B. *et al.* (2009) The clinical variability of maternally inherited diabetes and deafness is associated with the degree of heteroplasmy in blood leukocytes. *J. Clin. Endocrinol. Metab.*, **94**, 3025–3030.
20. Picard, M., Zhang, J., Hancock, S., Derbeneva, O., Golhar, R., Golik, P., O'Hearn, S., Levy, S., Potluri, P., Lvova, M. *et al.* (2014) Progressive increase in mtDNA 3243A>G heteroplasmy causes abrupt transcriptional reprogramming. *Proc. Natl. Acad. Sci. U. S. A.*, **111**, E4033–E4042.
21. McMillan, R.P., Stewart, S., Budnick, J.A., Caswell, C.C., Hulver, M.W., Mukherjee, K. and Srivastava, S. (2019) Quantitative variation in m.3243A > G mutation produce discrete changes in energy metabolism. *Sci. Rep.*, **9**, 5752.
22. Hayashi, J., Ohta, S., Kikuchi, A., Takemitsu, M., Goto, Y. and Nonaka, I. (1991) Introduction of disease-related mitochondrial DNA deletions into HeLa cells lacking mitochondrial DNA results in mitochondrial dysfunction. *Proc. Natl. Acad. Sci. U. S. A.*, **88**, 10614–10618.
23. Maeda, K., Kawai, H., Sanada, M., Terashima, T., Ogawa, N., Idehara, R., Makiishi, T., Yasuda, H., Sato, S., Hoshi, K. *et al.* (2016) Clinical phenotype and segregation of mitochondrial 3243A>G mutation in 2 pairs of monozygotic twins. *JAMA Neurol.*, **73**, 990–993.
24. Walker, M.A., Lareau, C.A., Ludwig, L.S., Karaa, A., Sankaran, V.G., Regev, A. and Mootha, V.K. (2020) Purifying selection against pathogenic mitochondrial DNA in human T cells. *N. Engl. J. Med.*, **383**, 1556–1563.
25. Hubner, A., Wachsmuth, M., Schroder, R., Li, M., Eis-Hubinger, A.M., Madea, B. and Stoneking, M. (2019) Sharing of heteroplasmies between human liver lobes varies across the mtDNA genome. *Sci. Rep.*, **9**, 11219.
26. Bentlage, H.A. and Attardi, G. (1996) Relationship of genotype to phenotype in fibroblast-derived transmitochondrial cell lines carrying the 3243 mutation associated with the MELAS encephalomyopathy: shift towards mutant genotype and role of mtDNA copy number. *Hum. Mol. Genet.*, **5**, 197–205.
27. Chichagova, V., Hallam, D., Collin, J., Buskin, A., Saretzki, G., Armstrong, L., Yu-Wai-Man, P., Lako, M. and Steel, D.H. (2017) Human iPSC disease modelling reveals functional and structural defects in retinal pigment epithelial cells harbouring the m.3243A > G mitochondrial DNA mutation. *Sci. Rep.*, **7**, 12320.
28. Jenuth, J.P., Peterson, A.C. and Shoubridge, E.A. (1997) Tissue-specific selection for different mtDNA genotypes in heteroplasmic mice. *Nat. Genet.*, **16**, 93–95.
29. Stewart, J.B., Freyer, C., Elson, J.L., Wredenberg, A., Cansu, Z., Trifunovic, A. and Larsson, N.G. (2008) Strong purifying selection in transmission of mammalian mitochondrial DNA. *PLoS Biol.*, **6**, e10.
30. Mariotti, C., Savarese, N., Suomalainen, A., Rimoldi, M., Comi, G., Prelle, A., Antozzi, C., Servidei, S., Jarre, L., DiDonato, S. *et al.* (1995) Genotype to phenotype correlations in mitochondrial encephalomyopathies associated with the A3243G mutation of mitochondrial DNA. *J. Neurol.*, **242**, 304–312.
31. Liu, G., Shen, X., Sun, Y., Lv, Q., Li, Y. and Du, A. (2020) Heteroplasmy and phenotype spectrum of the mitochondrial tRNA(Leu (UUR)) gene m.3243A>G mutation in seven Han Chinese families. *J. Neurol. Sci.*, **408**, 116562.
32. Scholle, L.M., Zierz, S., Mawrin, C., Wickenhauser, C. and Urban, D.L. (2020) Heteroplasmy and copy number in the common m.3243A>G mutation-a post-mortem genotype-phenotype analysis. *Genes (Basel)*, **11**, 212.
33. Tucker, B.A., Anfinson, K.R., Mullins, R.F., Stone, E.M. and Young, M.J. (2013) Use of a synthetic xeno-free culture substrate for induced pluripotent stem cell induction and retinal differentiation. *Stem Cells Transl. Med.*, **2**, 16–24.
34. Mullins, R.F., Kuehn, M.H., Faidley, E.A., Syed, N.A. and Stone, E.M. (2007) Differential macular and peripheral expression of bestrophin in human eyes and its implication for best disease. *Invest. Ophthalmol. Vis. Sci.*, **48**, 3372–3380.
35. Christopher, M., Moga, D.C., Russell, S.R., Folk, J.C., Scheetz, T. and Abramoff, M.D. (2012) Validation of tablet-based evaluation of color fundus images. *Retina*, **32**, 1629–1635.
36. Anderson, D.R. (1987) *Perimetry with and without Automation*. Mosby, St. Louis.
37. Weleber, R.G. and Tobler, W.R. (1986) Computerized quantitative analysis of kinetic visual fields. *Am J. Ophthalmol.*, **101**, 461–468.
38. Christoforidis, J.B. (2011) Volume of visual field assessed with kinetic perimetry and its application to static perimetry. *Clin. Ophthalmol.*, **5**, 535–541.